Acta of Bioengineering and Biomechanics
Vol. 21, No. 1, 2019

Original paper
DOI: 10.5277/ABB-01240-2018-04

Monitoring of the Achilles tendon healing process: can artificial intelligence be helpful?

NORBERT KAPIŃSKI[1]*, JAKUB ZIELIŃSKI[1, 2], BARTOSZ A. BORUCKI[1], TOMASZ TRZCIŃSKI[3, 5], BEATA CISZKOWSKA-ŁYSOŃ[4], URSZULA ZDANOWICZ[4], ROBERT ŚMIGIELSKI[6, 7], KRZYSZTOF S. NOWIŃSKI[1]

[1] Interdisciplinary Centre for Mathematical and Computational Modelling, University of Warsaw, Poland.
[2] Department of Biophysics and Human Physiology, Medical University of Warsaw, Poland.
[3] Faculty of Electronics and Information Technology, Warsaw University of Technology, Poland.
[4] Carolina Medical Center, Warsaw, Poland.
[5] Tooploox, Wrocław, Poland.
[6] MIRAI Institute: Trauma, Orthopaedics, Physical Therapy, Warsaw, Poland.
[7] ARS MEDICINALIS Foundation, Warsaw, Poland.

Purpose: The aim of this study was to verify improved, ensemble-based strategy for inferencing with use of our solution for quantitative assessment of tendons and ligaments healing process and to show possible applications of the method. *Methods:* We chose the problem of the Achilles tendon rupture as an example representing a group of common sport traumas. We derived our dataset from 90 individuals and divided it into two subsets: healthy individuals and patients with complete Achilles tendon ruptures. We computed approx. 160 000 2D axial cross-sections from 3D MRI studies and preprocessed them to create a suitable input for artificial intelligence methods. Finally, we compared different training methods for chosen approaches for quantitative assessment of tendon tissue healing with the use of statistical analysis. *Results:* We showed improvement in inferencing with use of the ensemble technique that results from achieving comparable accuracy of 99% for our previously published method trained on 500 000 samples and for the new ensemble technique trained on 160 000 samples. We also showed real-life applications of our approach that address several clinical problems: (1) automatic classification of healthy and injured tendons, (2) assessment of the healing process, (3) a pathologic tissue localization. *Conclusions*: The presented method enables acquiring comparable accuracy with less training samples. The applications of the method presented in the paper as case studies can facilitate evaluation of the healing process and comparing with previous examination of the same patient as well as with other patients. This approach might be probably transferred to other musculoskeletal tissues and joints.

Key words: *tendon traumas, magnetic resonance, medical imaging, artificial intelligence, deep learning*

1. Introduction

The injuries of tendons and ligaments are the most common musculoskeletal disorders in modern medical practice, with more than 18 case per 100 000 people per year [13]. The statistics translated to a Polish population gives the estimated number of 5890 people over 15 years of age injured every year. Moreover a risk of the tendon re-rupture is between 20–40%, i.e., 1000–2000 cases a year. Despite recent advances in the treatment of tendons and ligaments injuries, the question of an optimal one is still unanswered. Within this work we studied the Achilles tendon rupture problem as an example representing the whole group of sport injuries.

Medical professionals constantly work on novel treatment and rehabilitation protocols and techniques that could optimize the healing and rehabilitation time. The introduction of automated intelligent computer assistance tools, especially in radiology, can improve the diagnostic process, relieve the medical experts

* Corresponding author: Norbert Kapiński, ICM University of Warsaw, Tyniecka 15/17, 02-630, Warsaw, Poland. Phone: +48 22 87 49 337, e-mail: n.kapinski@icm.edu.pl
Received: November 6th, 2018
Accepted for publication: March 11th, 2019

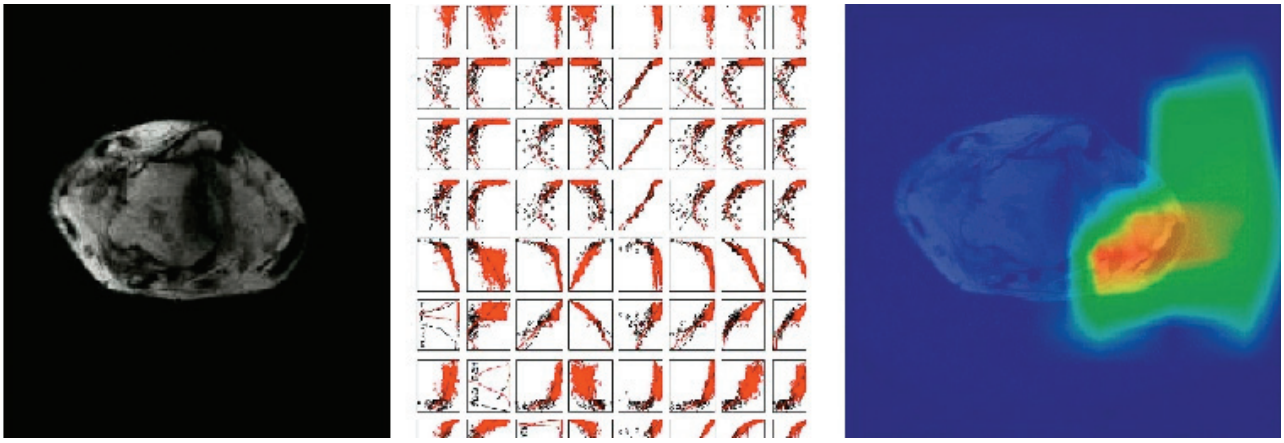

Fig. 1. The figure presents a workflow of the artificial intelligence based assessment of the Achilles tendon healing. First, numerical features are extracted from the input MRI image, then grouped into subsets (red – features of a healthy tendon, black – features of a ruptured one). Finally, the artificial intelligence method learns to depend on the features localized close to the tendon edema (focus represented by a heatmap)

from basic repeatable and labour-intensive tasks and serve as second or third opinion.

More precisely, in everyday practice evaluation of MRI images is subjective and radiologist-dependent. Computer science, especially artificial intelligence can provide methods for a quantitative and objective evaluation. As shown in Fig. 1, from medical images we extracted a number of numerical features that can differentiate problems like recognition of the Achilles tendon in particular phases of the healing.

A big advantage of the modern artificial intelligence methods is that features are extracted automatically based on a number of example images. Subsets of those features that describe the given problem best influence the final decision.

In this study, we focused on improving strategy for inferencing with use of our solution presented in [8], dedicated for quantitative assessment of tendons and ligaments healing process as well as showing possible applications of the method. First, we presented literature overview and recent advancements in medical image processing. Secondly, we described in details two well known models that we further use for improving our solution and also present case study applications. Within the case study we compare results of different tasks related to assessment of the healing of the Achilles tendon.

1.1. Deep learning in medical image processing

Due to the increasing number of layers stacked together to form neural networks, machine learning domain focused on using them to solve problems was dubbed *Deep Learning* (DL). Researchers have been successful in applying DL paradigm in the context of medical image processing. The first practical implementation of DL-like architecture in medical application appeared in 1993 in the work of Zhang [19]. The so-called shift-invariant networks were successfully used for screening mammography. Since then, rapid development of the field and wide interest of machine learning community in applying deep learning methods to medical data have enabled the algorithms to reach the performance of human experts in many domains. The authors of the paper [2] presented a skin cancer detection model that obtained classification results comparable with expert dermatologists opinions. In work [5], the authors proposed a DL system for diabetic retinopathy and diabetic macular edema detection which performance was comparable with an expert ophthalmologist. The most recent works prove that, in fact, human experts can even be outperformed in diagnostic accuracy by machine learning model. For instance, the authors of [18] proposed a deep learning method for identification and detection of metastatic breast cancer which improves over the accuracy of human pathologist's diagnoses. Similarly, [17] presents analogical work on recognition of the Alzheimer disease in MRI data. The authors of paper [3] have used machine learning algorithms to parcellated human cerebral cortex and [14] utilized deep neural networks to detect arrhythmia.

Convolutional Neural Networks

The most popular and successful class of deep neural networks models in image analysis applications are Convolutional Neural Networks (CNN's). The CNN's

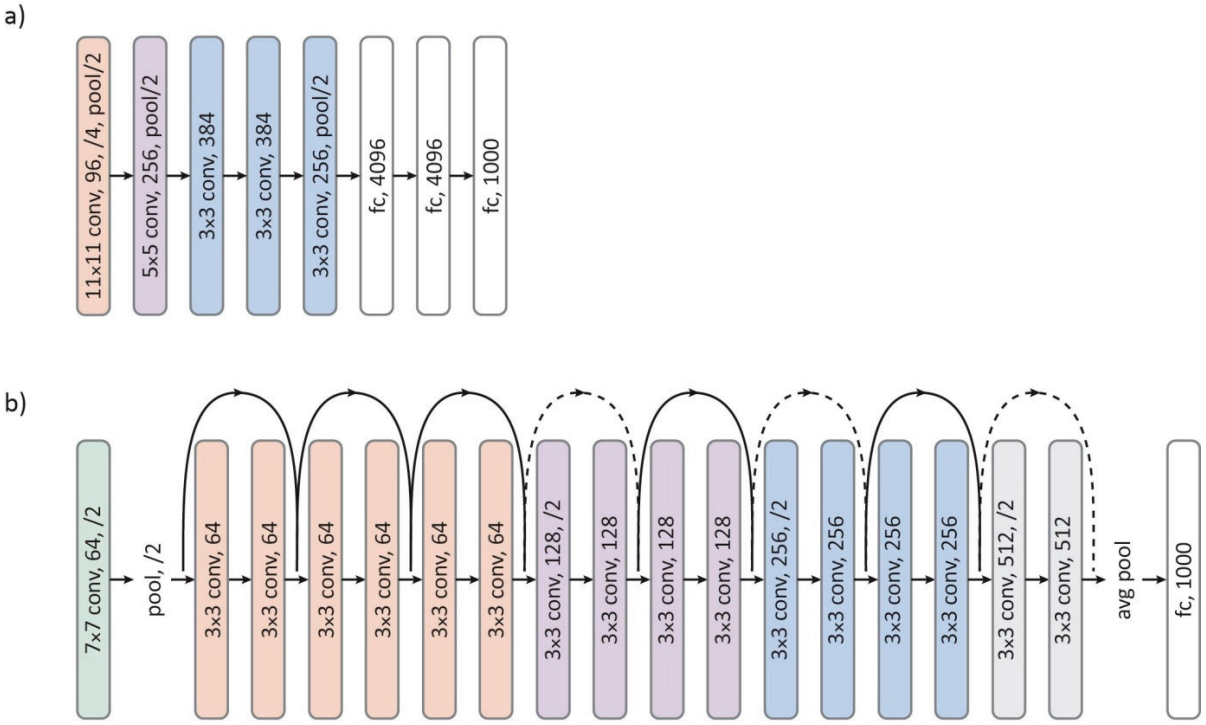

Fig. 2. Convolutional Neural Networks topologies used in the case study

topologies consist of connected building blocks which form a workflow and transform the input image into a prediction of belonging into a particular class (e.g., healthy or pathologic tissue). We decided to test two well known CNN architectures that differ in terms of number of layers, kernels for feature extraction and connectivity. The comparison of the selected AlexNet and ResNet topologies is presented in Fig. 2. The *AlexNet* (Fig. 2a) comprises of 3 max-pooling layers that follow respectively first, second and fifth of the five convolutional layers. The sizes of convolution filters in the subsequent convolutional layers are: 11×11, 5×5 and 3 times 3×3. The input image is downsized twice after each of the max-pooling layers and four times after the first convolutional layer which results from the value of a *stride parameter* (the image gap between subsequent convolutions) [10].

For comparison, the first stage of the ResNet-18 model (Fig. 2b) processes the image using 7×7 filters with stride 2, performs max-pooling and downsizes the result by a factor of 2. Further, there are 8 components performing residual mapping [6].

Regardless of differences, both architectures at the ends contain fully connected layers and a decision function which in our case is the *softmax function*, i.e.:

$$p_{nk} = \exp(x_{nk}) / [\sum_{k'} \exp(x_{nk'})]. \quad (1.1)$$

The softmax layer process a probability of belongings to different classes into the *final output*, a highly discretized answer (e.g., differentiating healthy from pathologic tissue). Based on a deeper analysis of particular parts of the presented models one can extract different mid-level features and produce continuously valued estimations suitable for a physiological process assessment, e.g., tendon or ligaments healing. Possible ensembles of the features imply an application to our problem, e.g., (as further shown) in terms of: (1) automatic classification of healthy and injured tendons, (2) assessment of the healing process, (3) a pathologic tissue localization.

2. Materials and methods

In this section, we presented several methods based on deep learning algorithms that enabled us to assess the healing process of the Achilles tendon. We first described the dataset used in the experiment. Then, we discussed data preparation and training protocol. Finally, we indicated how we trained and validated chosen deep neural networks.

2.1. Dataset

The dataset used in this work is created using Magnetic Resonance Imaging (MRI) images collected

within the frames of the START project "Novel Scaffold-based Tissue Engineering Approaches to Healing and Regeneration of Tendons and Ligaments". In this project, we acquired MRI data of a lower limb of 30 healthy volunteers and 60 patients after the Achilles tendon complete rupture with the use of a GE Signa HDxt 1.5T scanner with Foot & Ankle array coil. Healthy group was treated as a reference, while the patients followed a specially designed treatment after the tendon reconstruction.

To monitor the progress of the healing, each of the individuals was scanned with 10 most commonly used in orthopaedics (or, what is most interesting, in the image processing sense) MRI protocols, i.e., four 3D FSPGR Ideal [Fast Spoiled Gradient Echo] (In Phase, Out Phase, Fat, Water), PD [Proton Density], T1, T2, T2 mapping, T2* GRE [Gradient Echo] and T2* GRE TE_MIN [Minimal Time Echo].

The healthy group was scanned only once, while the injured patients were scanned once before the surgery and 9 times afterwards (after 1, 3, 6, 9, 12, 20, 26, 40 and 52 weeks). For the purpose of this work, we selected 500 3D MRI scans that contained data for healthy and injured patients (with equal proportion of each of the group). Figure 3 shows a sample 3D MRI image registered for an injured and healthy individual.

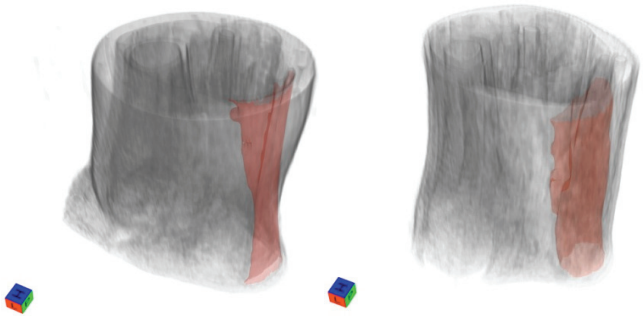

Fig. 3. Sample MRI PD protocol data volumetrically rendered with the healthy (left) and reconstructed (right) Achilles tendon marked in red

The data was visualised using VisNow software[1] developed at the Interdisciplinary Centre for Mathematical and Computer Modelling [12]. We applied volume rendering technique to the DICOM data and marked the Achilles tendon with the red colour.

2.2. Data preparation

Processing three-dimensional images with high resolution, such as 3D MRI scans, is computationally expensive and prone to artifacts introduced by data anisotropy (large distances between slices as compared to pixel size). Although several methods that analyse 3D images have been proposed [11], in this work we focused on 2D axial cross-sections of the 3D data points, also called *slices*, which enables faster computation, eliminates the need of data interpolations, reduces anisotropy artifacts and enables additional analysis including inter-protocol, e.g., in the context of validating influence of regenerative stem cell treatment. To this end, we used a multi-step data preparation pipeline, presented in Fig. 4.

First, we extracted over 45.000 slices representing the injured tendons and over 11.000 representing the healthy ones. For machine learning methods to perform at their best, the representation of samples of different classes should be balanced and represent realistic cases. Therefore, we augment the data by mirroring the slices and rotating the images twice by –5 and 5 degrees.

Mirroring allowed us to include approximate representations of opposite limbs, while small rotations balanced the dataset by adding cases representing variable healthy limb positions. The final dataset contains 159 770 slices.

We assigned binary labels of „healthy" and „injured" to all slices, depending on the condition of the patient. Furthermore, we performed random subsampling of the slices to make sure that during training CNNs do not learn on a series of similar cases, what could cause difficulties in finding a generic solution. We divided shuffled slices into a train, a test and a validation set, containing respectively 80, 10 and 10% of the total number of the slices. The sets were stored in the HDF5 format that naturally preserves the 16 bit range of MRIs data, so there was no need to recalculate values of the original units.

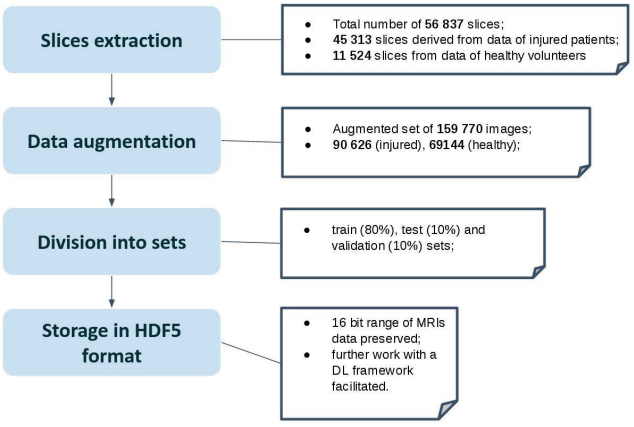

Fig. 4. Data preparation workflow

[1] http://visnow.icm.edu.pl

2.3. Training deep learning models

We used AlexNet and the ResNet-18 described in the introduction as our deep learning network architectures. We trained those architectures with a dataset of MRI data preprocessed according to the pipeline presented in the previous section. During the training phase, the network weights were updated by propagating the error made by the network on the training set. To monitor the error made by the network, we computed the accuracy on the test dataset. The training requires millions of parameters to be optimized, thus it is convenient to utilize novel computer architectures equipped with suitable accelerators, e.g., novel Graphical Processing Units (GPUs). A computational server with 4 NVIDIA M6000 GPUs with the CUDA v7.5 and the cuDNN v5.1 libraries was used for the purpose of this work. This configuration resulted in training times of around 40 minutes in case of the AlexNet and 7 hours in case of the ResNet-18.

On top of that, we used Caffe Berkeley deep learning framework, which was optimized for variety of hardware setups. One can find pre-trained deep learning models for Caffe framework (such as AlexNet and ResNet architectures used in this paper) in the Model-Zoo library. Although we used Caffe framework, one can find a multitude of other DL frameworks like TensorFlow, PyTorch or MXNet that can also be used to train deep learning models. In paper [1] a useful comparison of the DL frameworks was presented.

We conducted several initial experiments to validate the choice of training parameters. For example, during the training of the AlexNet we obtained the best classification accuracy gain by adjusting the step size parameter. In general, small step sizes, e.g., 250, tend to drive the optimization towards local minima, effectively stopping the progress of learning. In our case, increasing the step size to 2500 improved our classification accuracy by more than 11%. Due to the lack of progress in learning we stopped the training after 10 000 iteration in case of AlexNet and 120 000 iterations in case of the ResNet-18. Higher number of iterations needed to obtain optimal results for the ResNet architecture are caused by more complex architecture of this network.

2.4. Data classification

This stage is usually named the inference stage. The input data is propagated through the trained network and classified. Based on this results an accuracy of the model can be computed. For this purpose, we used the validation set. Validation set contains samples that haven't been previously shown to the model in neither training or testing process. That means that if the validation set is classified correctly, with high accuracy, then the learning process is successful.

Additionally to the inference based on the validation set, within this work we also performed a classification on subsets or full data sets again – to develop and formulate conclusions regarding the possible utilization of deep learning networks to the problem of monitoring of the Achilles tendon healing process. The reason for that approach was that we wanted to train the models with as much data as possible, however, to perform inference on a subset of the data that is suitable and most representing to the given case study. Details on the used training and inference data are given in the corresponding sections.

3. Results

In this section we presented results of a case study that comprises of three tasks. Firstly, we performed a binary classification. We used deep learning models to distinguish between healthy and injured images of the tendon and test several ensemble approaches to improve inferencing strategy. Secondly, we assessed the phase of the tendon healing with deeper analysis of the outputs of the tested models. Finally, we presented a proof of concept of a method of pathologic tissue localisation.

3.1. Automatic assessment of healthy and injured patient classes

Classification with the AlexNet and the ResNet-18 models

First, we evaluated our network on the task of binary classification. More precisely, we checked the accuracy of the network obtained when classifying the samples as healthy tendons or tendons after the trauma. We trained AlexNet and ResNet-18 models to classify slices in two groups: healthy and injured. Then we validated the results with the use of the validation set containing 10% of shuffled slices of all of the patients and all of the MRI protocols (Fig. 4). In Table 1 the results of our evaluation are presented.

Table 1. Results of the binary classification

Net	AlexNet (A)	ResNet-18 (B)
Iter. nr.	10 000	120 000
True healthy (TN)	7787	7944
True injured (TP)	7680	7623
False healthy (FN)	309	366
False injured (FP)	201	44
Correct detections (TP + TN)	15 467	15 567
Incorrect detections (FP + FN)	510	410
Set size	15 977	15 977
Sensitivity = TP/(TP + FN)	96.13%	95.41%
Specificity = TN/(TN + FP)	97.48%	99.45%
Accuracy = (TP + TN)/(Set Size)	96.81%	97.43%

The total accuracy score of the ResNet-18 (B) was only by 0.62% higher than the AlexNet (A) score.

Classification with an ensemble of the models

In our experiments we used softmax (Eq. (1.1)) as a decision function. For the problem described above, this setting resulted in close to certain predictions, i.e., the probability of a sample belonging to a given class is close to one. However, analyzing the results from the penultimate layer of our network, which we call the *network output* in the remainder of this section, we observe that the values changed in a more continuous manner. For all of slices derived from all of the patients scans, an average value of the output for AlexNet and ResNet models was respectively –4.12 and –3.45. Analogous results in the control group (healthy patients) were respectively 6.68 and 3.13.

The Spearman correlation coefficient between AlexNet output and ResNet output was equal to 0.79, while Spearman correlation coefficient between signs of the AlexNet and the ResNet outputs was equal to 0.88. That means that both networks were responding to the given input in the similar manner, but in some cases a synergy of the models could be more precise.

We, therefore, defined new decision functions which take advantage of combining model outputs. Firstly, we computed 2*NetsSign* = Signum(*2Nets*):

$$2Nets\sum_{j=0}^{n} y_j,$$

y_j is a neuron output value on the last fully connected layers of both used models. Furthermore, we trained an SVM classifier based on a sigmoidal kernel [4] also on both network outputs parameter space. Comparison of the accuracy values is presented in Table 2.

Table 2. Comparison of the tendon classification with use of the neural networks ensembles

	Sensitivity	Specificity	Accuracy
2NetsSign	98.3%	97.0%	97.2%
SVM	94.0%	98.6%	97.6%

We obtained the highest values of two of the three above presented parameters, i.e., *Accuracy* = 97.6% and *Specificity* = 98.6% for the ensemble with use of the SVM classifier. The highest *Sensitivity* = 98.3% was for the *2NetsSign*.

3.2. Assessment of the phase of the healing

After training the models with the binary labeled dataset, an information regarding features of the healthy and injured tendons was present within the feature extractor part of the CNN. We could therefore further optimize this model to allow for a proper classification of the healing stage given a MRI image as an input. We anticipated that the healed tendons contained more healthy features than the ones just before or just after the tendon reconstruction. The MRI inputs taken chronologically should lead to different outputs of the CNN models, which allowed us to monitor the progress of the healing process towards a healthy tendon. To validate our assumptions, we computed the average value of *2Nets* of two patients with 7 chronologically aligned studies in long-term recovery (6558 MRI slices in total). We chose to analyse PD protocol, as it is one of the 4 equally good protocols in terms of binary classification results presented by us in a separate study in [7]. Figure 5 shows the resulting average curve of this analysis.

Kruskal–Wallis one-way analysis of variance test show very high significance: $p < 0{,}001$***, H ($df = 6$, $N = 6558$) = 865. This means that value of the variable *2Nets* depends on the time after injury. The correlation between the mean values of the sequence number of an examination in the sequence of examinations performed during the healing process and the *2Nets* variable obtained from this MRI test was 0.91.

3.3. Pathologic tissue localisation

The localisation of the pathologic tissue can be done by simple extrapolation of the method presented for assessing current healing phase. Instead of computing the average of the CNN outputs for a particular 3D MRI study, one can plot the CNN outputs separately for each of the slices. The slices that contain

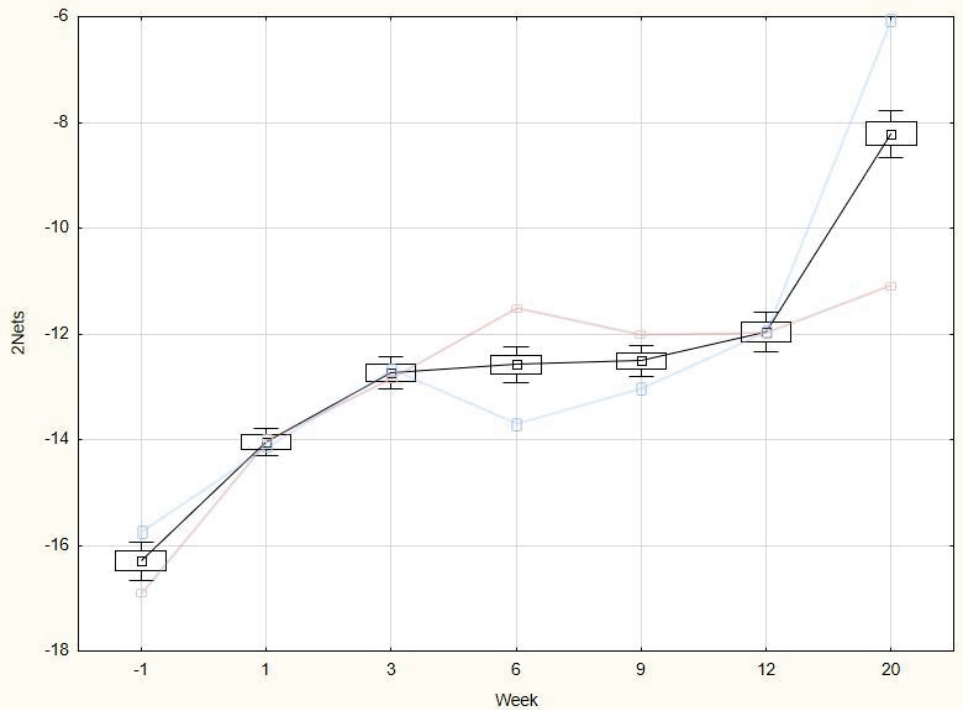

Fig. 5. Black line represent average values of the *2Nets* for all of the MRI cross-sections of two patients. The total number of images in the analysis is 6558. Box-whisker plot indicates mean, error of the mean and 95% confidence interval. Colour lines represents average values for single subjects

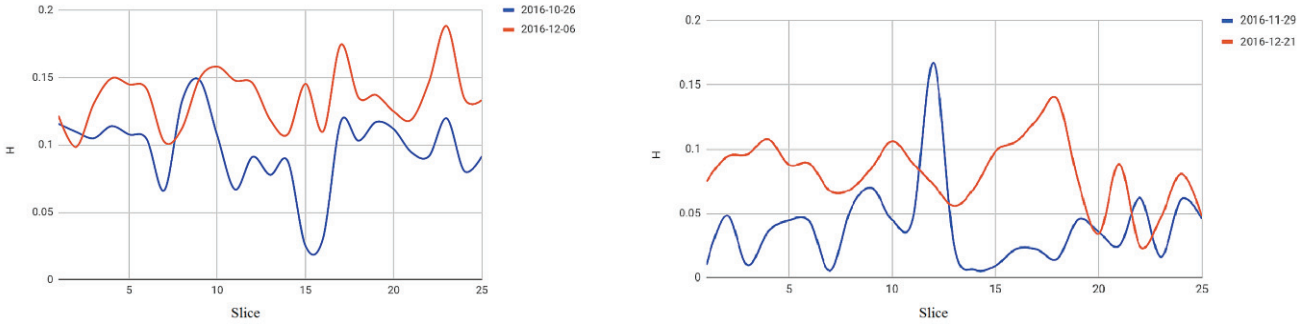

Fig. 6. Classification of the slices in the area of the rupture in two different phases of the therapy of the 2 patients

more features of the injured tendon should differ in output values from the ones that are similar to the healthy tendon. Again, to validate this assumption, for the same two patients studies presented in the previous section, we computed *H* defined as the output value of the healthy class given by the ResNet model (slightly better in terms of accuracy than the AlexNet). Figure 6 shows the slices in the area of the rupture in two different phases of the therapy of the 2 patients.

Blue curve represents slices score *H* just after the surgery, while the red curve indicates the score after 1–2 months of the rehabilitation. *X*-axis represents the slices number.

We performed Mann–Whitney *U*-test independently for each of the 2 patients and verified whether the change of measure *H* was statistically significant. The obtained *p*-values were: 0.000132 ***, 0.000004 ****, which proved the importance. Some of the mistakes can be also seen (e.g., slice 12 – Patient 2) where the output value did not follow the trend.

4. Discussion

We can state that both models (AlexNet and ResNet-18) perform equally well on a given task of the binary classification. However classification the ResNet-18 results in 152 more true healthy detections and 57 less true injured detections than the AlexNet. This fact indicates a possible chance of improvement with the use of an ensemble of the

models. Thus, we defined new decision functions and showed that the *2NetsSign* is an interesting method for distinguishing healthy slices of the tendon and for other applications *SVM*-based model ensemble provides the best results.

As an alternative or complementary method we can further use the fact that within slices labeled as injured, the appearance of a healthy tissue is possible when 3D MRI scan contains images of the tissue located far away from the rupture. The occurrence of false negative detections can be minimized based on a 3D analysis of the position of slices, e.g., slices located on the edges can be excluded from the study or introduced with weights or fuzzy class logic.

We showed that with the use of the models ensemble we can improve the binary classification parameters, however it is still not possible to assess the progress of the healing process. For this task, as it was pointed out, a deeper analysis of the continuous outputs of the fully connected layers was done. We introduced *2Nets* measure and showed that its value increases with subsequent examinations. The first period after the operation is the inflammation phase and during this time there is a significant increase of the measure. In the middle stage, the healing phase linked to tendon structuralization is chaotic thus we cannot observe any significant increase in the measure. Lastly, during the remodeling phase tendons are structurized and the measure again increase (Fig. 5).

In the last case study we applied the above described healing process assessment separately for each of the slices and showed a marked coincidence between localizations of the local minima and maxima of the CNN outputs for the two examinations at different phases of healing. This observation suggests that there is a correlation between the response of the CNN and the local status of the healing.

All of the results can be use to improve and enhance utilization of our method presented in [8]. Especially in terms of interpreting the neural network output for purpose of assessment of the healing phase and pathological tissue localisation. Furthermore the previous work showed binary classification of 99% achieved with a training set of approx. 500 000 cases. In this paper we achieved the same accuracy with the use of only ~160 000 cases. We can utilize this fact to further tune our solution and – what is even more important – to apply the ensemble technique to new (similar) scenarios like ACL healing monitoring, even with insufficient training data availability.

Finally, although there are existing quantitative descriptions of Achilles tendon rehabilitation after total rupture like: ATRS [9], VISA-A [15] or FAOS [16]. There are only suitable for measuring the general outcome, related to symptoms and physical activity of patients. There is no structurized description that could be applied to MRI studies of the Achilles tendon. Based on the presented studies we plan to formulate it in the future work and use a synergy of MRI and deep learning to detect side-to-side differences in tendon structure in individuals as well as tendon structure related to clinical performance.

5. Conclusions

A multitude of deep learning (DL) algorithms have been proposed recently, many of them proved successful when applied to medical images. In the paper we hypothesize in what areas Convolutional Neural Networks (CNNs) – a subset of DL – can support treatment of tendon as well as, due to structural similarity, ligaments. More precisely, we analysed two well known CNN topologies (AlexNet and ResNet-18) to validate their usefulness to the problem of Achilles tendon healing assessment, monitored after rupture, one of the most common injuries in sport.

First, we tested the accuracy of the two CNNs in order to distinguish healthy tendons from injured ones. Both topologies performed equally well in the task resulting in accuracy of approximately 97%. We also showed that this result can be further slightly improved with ensemble of the models. We hypothesize that this method can be used in practice, e.g., to objectively compare the treatment duration and impact. It also can be utilized to improve inferencing results of our existing method or applied as a core of similar solutions, when proper amount of data is unavailable.

Secondly, we analyzed the possibility of developing the tendon healing score formulated based on outputs of intermediate CNN layers. We obtained a significant functional correlation that suggests a possible continuous valued estimations in a form of healing curves. Further we also hypothesize that physicians can use this information to perform precise, patient-specific assessment of the healing phase and invoke particular procedures at the appropriate time.

Finally, we presented a method for pathologic tissue localization. This time we developed healing scores for individual slices. The presented results showed significant correlation between localization of the local minimas and maximas. In practice, those healing scores can be used to objectively differentiate tissue state and

to point out proper place of healing stimuli implementation, e.g., stem cells.

We can conclude that deep learning methods can support the problem of quantitative tendons and ligaments healing assessment in multiple manner. For future work, a strict cooperation with the medical professionals is planned to validate this hypothesis and formulate a structurized description that could be applied to MRI studies of the Achilles tendon.

Acknowledgments

The following work was part of "Novel Scaffold-based Tissue Engineering Approaches to Healing and Regeneration of Tendons and Ligaments (START)" project, co-funded by The National Centre for Research and Development (Poland) within STRATEGMED programme (STRATEGMED1/233224/10/NCBR/2014).

References

[1] BAHRAMPOUR S., NAVEEN RAMAKRISHNAN, SCHOTT L., SHAH M., *Comparative Study of Caffe, Neon, Theano, and Torch for Deep Learning*, Computer Research Repository, 2015, abs/1511.06435.

[2] ESTEVA A., KUPREL B., NOVOA R.A., KO J., SWETTER S.M., BLAU H.M., THRUN S., *Dermatologist-level classification of skin cancer with deep neural networks*, Nature, 2017, Vol. 542, No. 7639, 115–118.

[3] GLASSER M.F., COALSON T.S., ROBINSON E.C., HACKER C.D., HARWELL J., YACOUB E., UGURBIL K., ANDERSSON J., BECKMANN C.F., JENKINSON M., SMITH S.M., VAN ESSEN D.C., *A multi-modal parcellation of human cerebral cortex*, Nature, 2016, Vol. 536, No. 7615, 171–178.

[4] GOEL A., SRIVASTAVA S.K., *Role of Kernel Parameters in Performance Evaluation of SVM*, Second International Conference on Computational Intelligence & Communication Technology, Ghaziabad, 2016, 166–169.

[5] GULSHAN V., PENG L., CORAM M., STUMPE M.C., WU D., NARAYANASWAMY A., VENUGOPALAN S., WIDNER K., MADAMS T., CUADROS J., KIM R., RAMAN R., NELSON P.Q., MEGA J., WEBSTER D., *Development and validation of a deep learning algorithm for detection of diabetic retinopathy in retinal fundus photographs*, Journal of the American Medical Association, 2016, arXiv:1803.04337.

[6] HE K., ZHANG X., REN S., SUN J., *Deep residual learning for image recognition*, Conference on Computer Vision and Pattern Recognition, 2016, 770–778.

[7] KAPIŃSKI N., ZIELIŃSKI J., BORUCKI B., NOWIŃSKI K.S., *MRI-based deep learning for in-situ monitoring of achilles tendon regeneration process*, International Journal of Computer Assisted Radiology and Surgery, 2017, Vol. 12, 57–58.

[8] KAPIŃSKI N., ZIELIŃSKI J., BORUCKI B., TRZCIŃSKI T., CISZKOWSKA-LYSON B., *Estimating Achilles tendon healing progress with convolutional neural networks*, Proceedings of the Medical Image Computing and Computer Assisted Intervention, 2018, arXiv:1806.05091.

[9] KEARNEY R., ACHTEN J., LAMB S., PARSONS N., COSTA M.L., *The Achilles tendon total rupture score: a study of responsiveness, internal consistency and convergent validity on patients with acute Achilles tendon ruptures*, Health and quality of life outcomes, 2012, Vol. 10, 24–29.

[10] KRIZHEVSKY A., SUTSKEVER I., HINTON G.E., *Imagenet classification with deep convolutional neural networks*, Conference on Neural Information Processing Systems, 2012, 25, 1097–1105.

[11] MILLETARI F., NAVAB N., *V-Net: Fully Convolutional Neural Networks for Volumetric Medical Image Segmentation*, Computer Research Repository, 2016, http://arxiv.org/abs/1606.04797.

[12] NOWIŃSKI K.S., BORUCKI B., *VisNow a Modular, Extensible Visual Analysis Platform*, Proc. of 22nd Int. Conf. in Central Europe on Computer Graphics, Visualization and Computer Vision WSCG2014, 2014, 73–76.

[13] RAIKIN S., GARRAS D.N., KRAPCHEV P.V., *Achilles Tendon Injuries in a United States Population*, Foot & Ankle International, 2013, 34, 475–480.

[14] RAJPURKAR P., HANNUN A.Y., HAGHPANAHI M., BOURN C., NG A.Y., *Cardiologist-Level Arrhythmia Detection with Convolutional Neural Networks*, Computer Research Repository, 2017, Vol. abs/1707.01836.

[15] ROBINSON J.M., COOK J.L., PURDAM C., VISENTINI P., ROSS J., MAFFULLI N., TAUNTON J., KHAN K., *The VISA-A questionnaire: a valid and reliable index of the clinical severity of Achilles tendinopathy*, British Journal of Sports Medicine, 2001, Vol. 35, 335–341.

[16] ROOS E.M., BRANDSSON S., KARLSSON J., *Validation of the Foot and Ankle Outcome Score for Ankle Ligament Reconstruction*, Foot & Ankle International, 2001, Vol. 22, 788–794.

[17] SARRAF S., TOFIGHI G., *Deep learning-based pipeline to recognize alzheimer's disease using fmri data*, IEEE Future Technologies Conference, 2016, 816–820.

[18] WANG D., KHOSLA A., GARGEYA R., IRSHAD H., BECK A.H., *Deep Learning for Identifying Metastatic Breast Cancer*, Computer Research Repository, 2017, arXiv:1606.05718.

[19] ZHANG W., DOI K., GIGER M.L., WU Y., NISHIKAWA R.M., SCHMIDT R.A., *Computerized detection of clustered microcalcifications in digital mammograms using a shift-invariant artificial neural network*, Medical Physics, 1994, Vol. 21, 517–524.